International Journal of Machine Tools & Manufacture 66 (2013) 95–101

Contents lists available at SciVerse ScienceDirect

International Journal of Machine Tools & Manufacture

journal homepage: www.elsevier.com/locate/ijmactool

Short Communication

Modeling of radial gap formed by material dissolution in simultaneous micro-EDM and micro-ECM drilling using deionized water

Minh Dang Nguyen*, Mustafizur Rahman, Yoke San Wong

National University of Singapore, Department of Mechanical Engineering, 9 Engineering Drive 1, 117576, Singapore

ARTICLE INFO

Article history:
Received 27 July 2012
Received in revised form
5 December 2012
Accepted 10 December 2012
Available online 25 December 2012

Keywords:
Micro-EDM
Micro-ECM
Deionized water
Short pulses
Modeling
Radial gap

ABSTRACT

For enhancing the surface finish of micro-holes, micro-EDM and micro-ECM have been combined in a unique hybrid machining process by using low-resistivity deionized water as bi-characteristic fluid. The affected material layer generated by electric sparks is further dissolved from machined surface owing to the effect of electrochemical reaction. To maintain the dimensional accuracy of micro-holes, short voltage pulses are applied to localize the material dissolution zone and thus the thickness of further removed material layer is of prime importance in deciding the final dimension of micro-holes. This study presents the modeling of radial gap distance in simultaneous micro-EDM and micro-ECM drilling by predicting the thickness of material layer further dissolved by electrochemical reaction. The analytical approach incorporating the double-layer theory, the Butler–Volmer equation and the Faraday's law of electrolysis is used to simulate the radial gap distance for different pulse parameters. The simulation data is then verified with the experimental results. It is observed that the applied pulse parameters directly affect the final dimension of obtained micro-holes. The effectiveness of short voltage pulses in localizing the material dissolution zone is found to be in accordance with the double-layer charging characteristic. When the pulse duration is too short, the material dissolution is negligible and SEDCM has no effect on improving the inner surface of micro-hole.

1. Introduction

Owing to the remarkable advantage which is negligible cutting force, micro-electric discharge machining (micro-EDM) is a preferable process for machining micro-shapes [1,2]. However, micro-EDM still has some disadvantages which stem from its own material removal mechanism. Because the material is removed through melting and vaporization, the machined surface is made up with thermally damaged layers [3,4]. The uppermost layer, which has been known as the white layer or recast layer, has high residual stress and may contain micro-cracks. Beneath this recast layer are the other heat affected zones which undergo material structure alteration. In addition, the texture of generated surface is characterized by the overlapping of numerous discharge craters which usually associates with high irregularities [5].

The enhancement of surface generated by micro-EDM is thus highly desirable. For improving the surface integrity of machined shapes, electrochemical micromachining (micro-ECM) has been combined as a sequential process after micro-EDM. Because the material removal mechanism is based on the ionic dissolution, the surface generated by micro-ECM is relatively smooth and free of residual stress as well as micro-crack [6]. This approach has also been studied in several researches [7–10]. The results from these studies demonstrate that ECM could be used as an effective method to reduce the roughness of surfaces generated by EDM. For small-size products and micro-scale applications, the solution with significantly low conductivity such as deionized water has been used as a weak electrolyte in enhancing the surface finish of micro-shapes by micro-ECM. The lateral surface integrity of micro-pin and micro-hole has been reported to be enhanced by some researchers [11,12]. Although such low conductivity solution has been used to moderate dissolution rate, the stray material dissolution is a challenging issue for micro-machining. It is realized that when being exposed to long dissolution time or using significantly low resistivity deionized water, the machined shapes is distorted due to the excessive material removal by electrochemical reaction [12,13]. Recently, the EDMed surface of micro-shapes has also been improved by performing micro-ECM right after micro-EDM [14]. Although they are carried out in the same machine tool, the machining fluid needs to be changed from dielectric fluid to electrolyte and different power supply is also required for micro-ECM.

In that scenario, micro-EDM and micro-ECM have been combined in a unique machining process, known as simultaneous micro-EDM and micro-ECM (SEDCM), to produce micro-shapes with better surface integrity [15,16]. In this method, low-resistivity

* Corresponding author. Tel.: +6516 4644.
E-mail addresses: dang@nus.edu.sg, nmdang85@yahoo.com (M.D. Nguyen), mpemusta@nus.edu.sg (M. Rahman), mpewys@nus.edu.sg (Y.S. Wong).

0890-6955/$ - see front matter © 2012 Elsevier Ltd. All rights reserved.
http://dx.doi.org/10.1016/j.ijmachtools.2012.12.001

deionized water is used as bi-characteristic fluid. The exceeding material dissolution which is considered as the disadvantage of micro-EDM using deionized water is now exploited in such a way that it is controlled and limited within a certain area. To obtain that objective, short voltage pulses have been used to localize the material dissolution zone. With different pulse parameters, the radial gap has been reported to be varied resulting in the difference in diameter of micro-holes [15]. Hence, this study attempts to perform the modeling of radial gap distance in simultaneous micro-EDM and micro-ECM drilling by predicting and simulating the thickness of affected material layer further removed by electrochemical reaction. The analytical approach used in this study originates from the double-layer theory, the Butler–Volmer equation and the Faraday's law of electrolysis.

2. Theoretical analysis

2.1. Radial gap model

In conventional micro-EDM drilling, material is removed by the discharge through melting and vaporization. Therefore, the machining gap formed is constituted of the critical distance and the discharge depth [17]. However, in SEDCM drilling, a thin layer of affected material on the lateral surface generated by the sparks is further removed to enhance the surface integrity of micro-hole, as illustrated in Fig. 1. As a result, aside from the critical distance and the discharge depth, the radial gap in this hybrid process also consists of the dissolution depth which stems from the electrochemical reaction. For the critical distance and the discharge depth, due to the stochastic nature of electrical breakdown in dielectric liquids, there has been no robust understanding of the electrical discharge [18,19]. Therefore, the breakdown strength of dielectric and the spark gap after EDM process are usually obtained by empirical methods. Moreover, the final radial gap in SEDCM drilling is dependent on the thickness of material layer which is further dissolved by electrochemical reaction. Hence, this model focuses on the material dissolution characteristic after the discharge to perform the modeling of radial gap of obtained micro-holes. For that reason, the side gap formed after micro-EDM is considered as the initial gap for material dissolution. In addition, the average surface roughness caused by overlapping discharge craters (around 0.142 μm R_a) is significantly smaller than the side gap after micro-EDM (about 5 μm) [16]. Hence, the roughness of surface generated by micro-EDM could be neglected when modeling the gap distance.

Owing to the slight conductivity of low-resistivity deionized water, it could be considered as a weak electrolyte and thus the side gap between electrode and workpiece could be modeled as an electrochemical cell. When a voltage is applied across two electrodes immersed in deionized water, the ions in the solution move towards electrode surface and the double layer is formed at the interface of electrode and electrolyte. It was reported that this electrode–solution interface behaves as a two parallel plate capacitor [20,21]. Thus, it could be modeled as a capacitor, as shown in Fig. 2 [22,23]. In this model, R_{sol} is the resistivity of deionized water. The C_{DL}' and C_{DL}'' are the capacitance of double layer at the electrode and workpiece surfaces respectively. Similarly, the R_F' and R_F'' are the Faradic resistance (or transfer resistance) representing the current density of electrochemical reaction at the surfaces of electrode and workpiece. Because the thickness of the double layer is significantly smaller than the radial gap distance, the solution resistance R_{sol} could be expressed as follows:

$$R_{sol} = \rho d_g \tag{1}$$

where ρ is the specific resistivity of deionized water and d_g is the electrode–workpiece distance.

2.2. Polarization of double layer

Prior to model development, certain assumptions are made for this study:

- The capacitance of double layer is constant during machining process.
- The transfer resistance and the capacitance of double layer at the electrode–solution and workpiece–solution interfaces are the same ($R_F' = R_F'' = R_F$ and $C_{DL}' = C_{DL}'' = C_{DL}$).
- There is no material dissolution during pulse-off time.
- The surface roughness of electrode and workpiece surface is neglected in simulating the radial gap distance.

Following the model in Fig. 2, the current density flowing through the workpiece–electrolyte interface comprises two routes: the charging current density i_C (to charge the double layer capacitance C_{DL}) and the Faradic current density i_F (flows through the transfer resistance R_F).

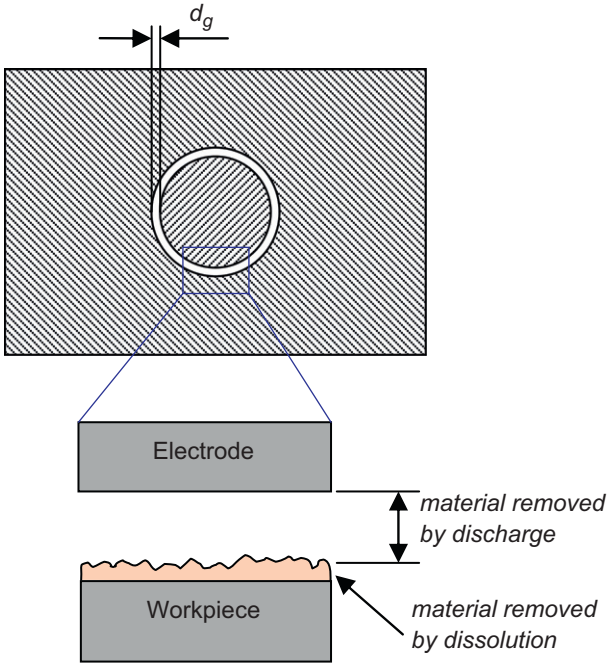

Fig. 1. Illustration of the radial gap in SEDCM drilling.

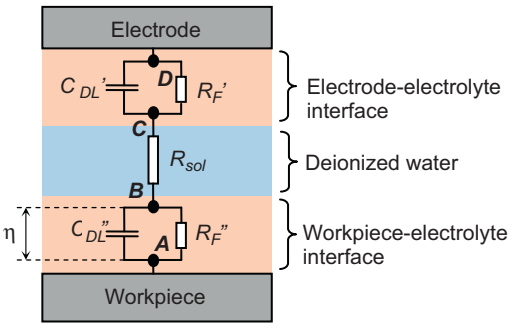

Fig. 2. Model of electrode–workpiece side gap in terms of circuit element.

The charging current density i_C is given by the equation:

$$i_C = C_{DL}\frac{d\eta}{dt} \tag{2}$$

in which t is the time variable and η is the double layer polarization

It has been reported that the Faradic current density is exponentially dependent on the potential drop between the double layer. Hence, originating from the Butler–Volmer equation [21], the Faradic current density is given by the following equation:

$$i_F = i_o[\exp(\alpha zf\eta) - \exp(-\alpha zf\eta)] \tag{3}$$

where i_o is the exchange current density at the equilibrium condition, α is the transfer coefficient, z is the number of electrons exchanged during electrochemical reaction and

$$f = F/RT \tag{4}$$

in which F is the Faraday constant, R is the gas constant and T is the absolute temperature.

In Eq. (3), the former term corresponds to the anodic current density whereas the latter term refers to the cathodic current density. These anodic and cathodic reactions happen on the same electrode. In the application which exploits the anodic dissolution of metal, the over-potential η is considerably high and thus the cathodic current density is significantly small. Therefore, it can be neglected and the Faradic current density flows through the transfer resistance R_F could be simplified to be

$$i_F = i_o\exp(\alpha zf\eta) \tag{5}$$

hence, the current density flowing from node A to B is given by equation:

$$I_{AB} = C_{DL}\frac{d\eta}{dt} + i_o\exp(\alpha zf\eta) \tag{6}$$

The current density flowing from node B to C is calculated as follows:

$$I_{BC} = \frac{U - U_{AB} - U_{CD}}{R_{sol}} = \frac{U - 2\eta}{\rho d_g} \tag{7}$$

where U is the amplitude of applied voltage pulses.

Here $I_{AB} = I_{BC}$, so it can be derived:

$$\frac{d\eta}{dt} = \frac{1}{C_{DL}}\left(\frac{U - 2\eta}{\rho d_g} - i_o\exp(\alpha zf\eta)\right) \tag{8}$$

Now, the polarization of double layer η could be obtained. From that, the current density i_F could be determined using Eq. (5).

2.3. Determination of dissolution rate

In order to calculate the dissolution rate, the current density needs to be determined. However, in this process, the short voltage pulses are applied instead of the continuous voltage. Therefore, the average current density must be calculated through the total electric charge per unit area q. During one pulse, the total electric charge per unit area passing through the substance could be determined by integrating the current density i_F over the pulse-on time t_{on}:

$$q = \int_0^{t_{on}} i_F dt \tag{9}$$

Eq. (9) yields the total electric charge per unit area passing per single voltage pulse. Therefore, the average current density per second could be obtained by dividing the total electric charge per unit area by the pulse period t_p as expressed in equation

$$i_a = \frac{q}{t_p} \tag{10}$$

in which

$$t_p = 1/frequency \tag{11}$$

Then, originating from the Faraday's law of electrolysis [21], the average dissolution rate per second is given by the following equation

$$v = \frac{i_a M}{zF} \tag{12}$$

where M is the molar volume of workpiece material.

2.4. Simulation of radial gap distance over time

From Eqs. (5) and (8), it can be seen that the current density is a function of the electrode–workpiece radial gap d_g. When the gap increases, the current density is slightly smaller and thus the dissolution rate is changed. Hence, to simulate the change of radial gap over time, the iteration method shown in Fig. 3 was used to update the new dissolution rate after each time step Δt.

3. Simulation results

The simulation works were carried out to investigate the effects of different pulse parameters on the radial gap formed during machining process. The simulation parameters used in this study are shown in Table 1.

The initial gap is set to be the spark gap when the electrochemical reaction is mostly suppressed, which is experimentally obtained to be approximately 5 μm. The exchange current density is the current density at the equilibrium condition of which the net current is zero. In other words, at equilibrium there is a balance of anodic and cathodic reaction happening at the same electrode surface. It is given that this exchange current density

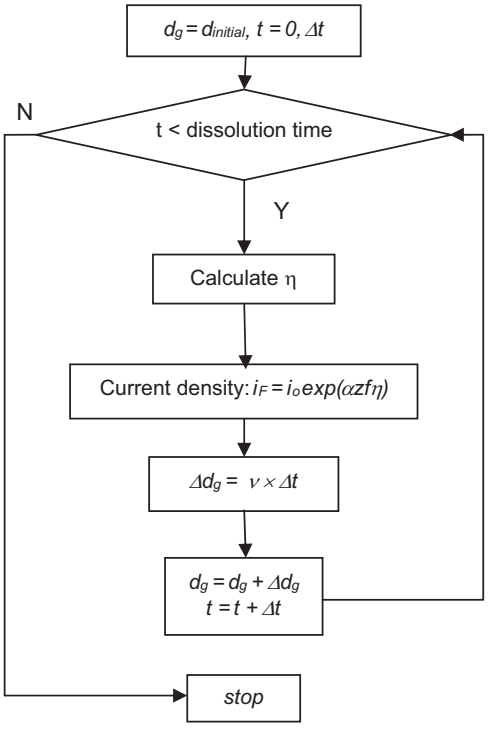

Fig. 3. Iterative algorithm to simulate the change of radial gap.

could be as high as 10 A/cm^2 or smaller than 1 pA/cm^2 [21]. In this study, partially deionized water which can be considered as a weak electrolyte is used. Therefore, the exchange current density is chosen to be 70 μA/cm^2. Besides, the capacitance of double layer is typically ranged from 10 to 40 μF/cm^2 [21]. However, it is reported that for the dilute electrolyte, the double layer capacitance significantly drops from 7 μF/cm^2 for 10 mM H_2SO_4 to 1.2 μF/cm^2 for 1 mM H_2SO_4 [22]. For low-resistivity deionized water, it could be seen as a very dilute electrolyte and the double layer capacitance is selected to be 0.5 μF/cm^2 in this simulation.

Table 1
Simulation parameters.

Initial gap distance, $d_{initial}$ (μm)	5
Specific conductivity of solution, ρ (MΩ cm)	0.4
Double layer capacitance, C_{DL} (μF/cm^2)	0.5
Transfer coefficient, α	0.5
Valency number of ions, z	2
Faraday constant, F (C mol^{-1})	96485
Gas constant, R (J mol^{-1} K^{-1})	8.314
Temperature, T (Kelvin)	298.15
Exchange current density, i_o (μA/cm^2)	70
Pulse amplitude, U (V)	60
Pulse frequency (kHz)	100, 300, 500
Pulse duty ratio	0.15–0.9
Molar volume, M (cm^3/mol)	7.11
Time step, Δt (s)	10
Dissolution time (s)	300

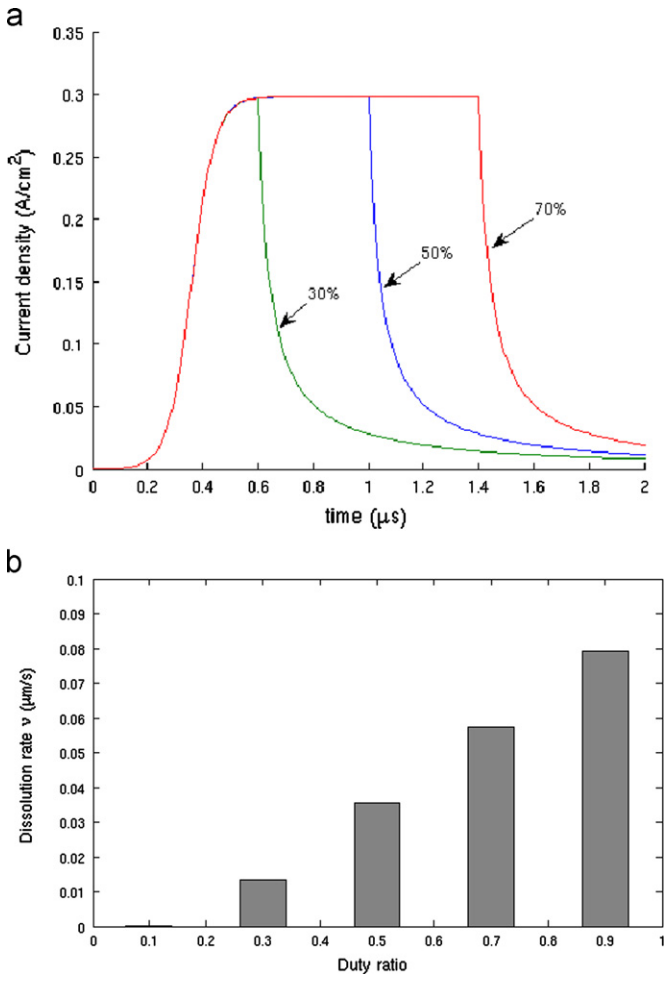

Fig. 4. Simulation of current density (a) and dissolution rate (b) for different duty ratios (*frequency*=500 kHz, $d_{initial}$=5 μm).

3.1. Effect of duty ratio

Fig. 4a exhibits the simulated data of current density for different duty ratios during one pulse period. In this case, the frequency is set at 500 kHz so the pulse period is calculated to be 2 μs. It is noteworthy that during the first 0.3 μs, although the

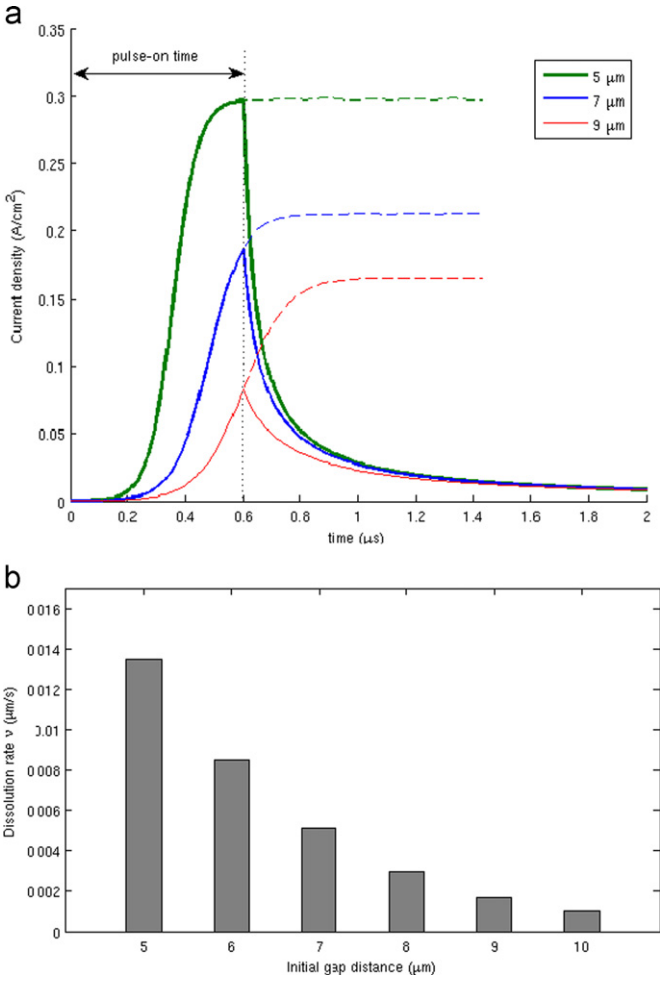

Fig. 5. Simulation of current density (a) and dissolution rate (b) for different initial gap distance (*frequency*=500 kHz, *duty ratio*=0.3).

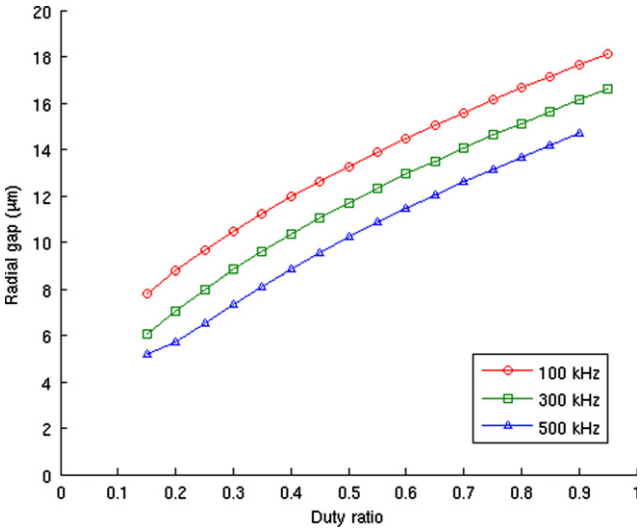

Fig. 6. Simulation of radial gap distance for different frequencies and duty ratios ($d_{initial}$=5 μm).

voltage has been applied but the current density remains steady near zero. Then, it has the sharp rise to reach the peak 0.3 A/cm^2 at 0.6 μs. This is attributed to the double layer charging characteristic. When the voltage is applied, the ions in the solution move towards the workpiece surface to form the double layer. The Faradic current is exponential dependent on the polarization of this double layer, as indicated in Eq. (5). It takes certain time for double layer to be fully charged so the Faradic current merely remains near zero at the beginning and increases sharply after 0.3 μs. When the current density peaks and keeps stable at 0.3 A/cm^2, it is indicated that the double layer is fully charged.

It can also be observed that with the smaller duty ratio (or shorter pulse-on time), the width of current density profile becomes thinner. After the pulse-on time duration, the applied voltage drops to zero and thus the current falls off. In addition, the dissolution rate is dependent on the total charge transferred during one pulse, as indicated in Eq. (9). Therefore, higher duty ratio would result in higher dissolution rate, as plotted in Fig. 4b. It is also noted that when the duty ratio is too small, the dissolution rate is negligible because the pulse-on time is too short for the double layer to be significantly charged. This is the situation in which there is no visible effect of material dissolution to improve the surface finish of micro-hole.

3.2. Effect of gap distance

Fig. 5a shows the simulated data of current density for different initial gap distance during one pulse period. The pulse frequency and duty ratio are fixed at 500 kHz and 0.3 respectively.

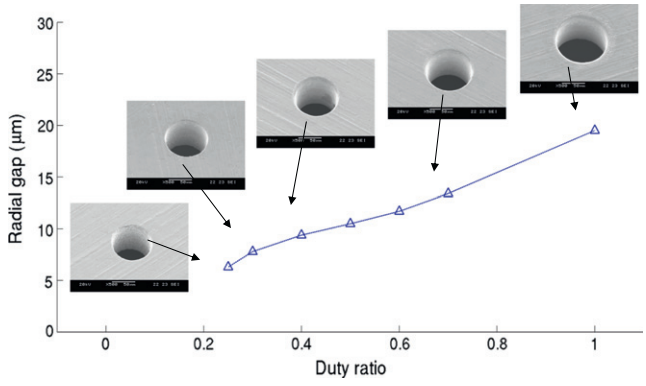

Fig. 7. SEM images and radial gaps of micro-holes corresponding to different pulse duty ratios (*frequency*=500 kHz).

It could be seen that the current density could reach the peak for 5-μm gap. It means that the double layer is considered to be fully charged. On the contrary, it is observed that for higher gap distance (7 and 9 μm), the current density is reduced and it could not even reach the peak value. This is due to the fact that 0.6 μs pulse-on-time is not long enough for the double layer to be fully charged. As a result, the dissolution rate is significantly reduced for higher gap distance, as indicated in Fig. 5b. This explains how the material dissolution is localized and thus the dimensional accuracy is improved when short voltage pulses are used.

3.3. Effect of pulse frequency

Fig. 6 simulates the radial gap distance for different duty ratios ranging from 0.15 to 0.9 and for three frequencies: 100, 300 and 500 kHz. It can be observed that at the same frequency, higher duty ratio would result in bigger radial gap. This is the results of the characteristics explained in Sections 3.1 and 3.2. With longer pulse-on time, the total electric charge per pulse is higher and thus the material is dissolved more. In addition, longer pulse duration would allow the double layer to be fully charged at higher gap distance. As a result, the material dissolution could occur for further range and thus it results in bigger diameter of micro-hole.

It is also observed that at the same duty ratio, higher frequency would result in smaller radial gap distance. This is the consequence of shorter pulse-on time. As we know, the pulse-on time is the product of pulse period and duty ratio. With higher pulse frequency, the pulse period is smaller as indicated in Eq. (11). For that reason, the pulse on-time is shorter leading to the limitation of dissolution range. That is the reason why at the same duty ratio, the diameter of micro-hole is predicted to be smaller for higher frequency.

4. Experimental verification

From the simulation results, it could be seen that the pulse parameters directly affect the radial gap of machined micro-holes. Hence, the simulated data obtained in Section 3.3 is compared with the experimental results obtained from previous study [15], whereby the effects of pulse frequency and duty ratio are demonstrated. In addition, the effectiveness of short voltage pulses in localizing the dissolution zone is also verified by investigating the change of radial gap when exposing to long dissolution time.

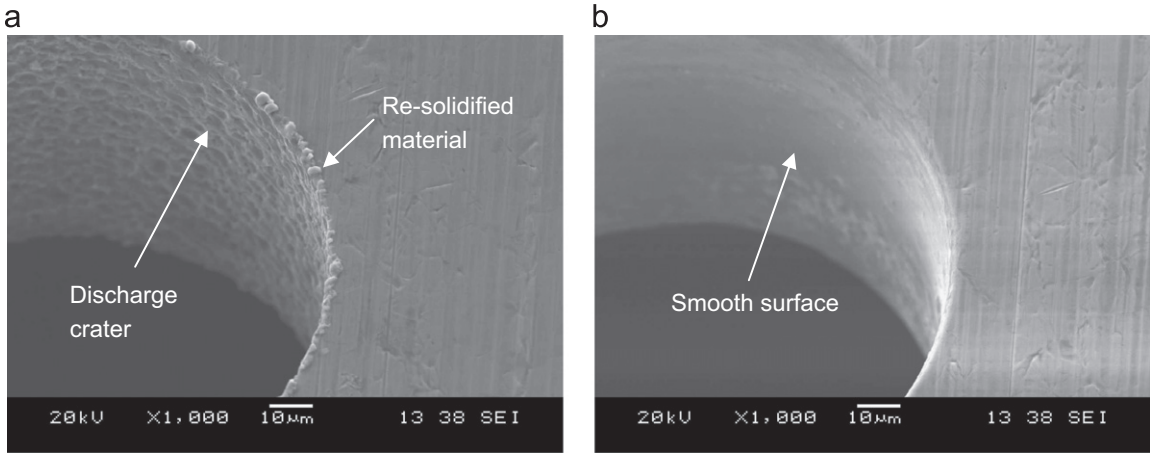

Fig. 8. SEM images of micro-holes fabricated without (a) and with (b) the effect of material dissolution.

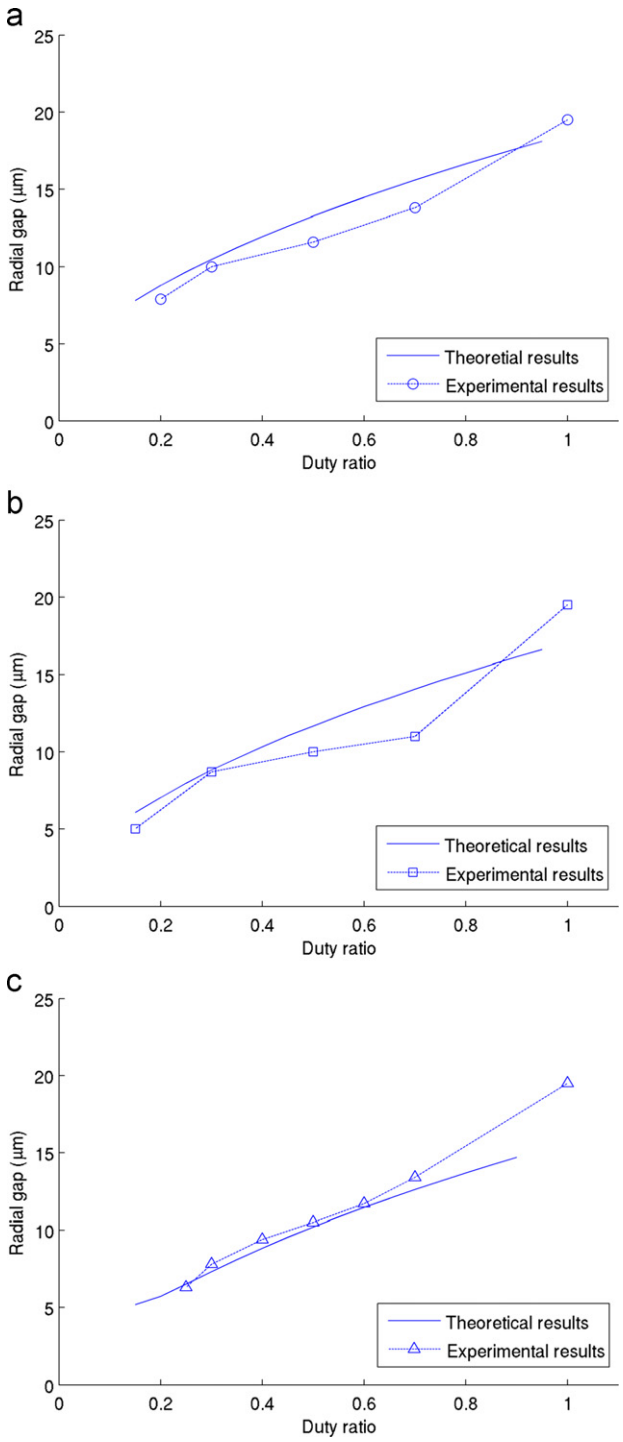

Fig. 9. Comparison of experimental data and simulated results of radial gap for different pulse frequencies: (a) 100 kHz, (b) 300 kHz and (c) 500 kHz.

Fig. 7 shows the radial gap and the SEM images of micro-holes fabricated using 500 kHz pulse for different duty ratios. It can be observed that the micro-hole is larger when higher duty ratio is used. Especially, at the duty ratio of 0.25, it is noted that the lateral surface of micro-hole is mostly covered with the overlapping discharge crater. This is the situation that has been explained in the Section 3.1. Since the pulse-on time is too short, the double layer could not be significantly charged even for the initial gap generated by the sparks, which results in the negligible dissolution rate. As a result, the irregular recast layer generated by electric sparks is not effectively removed from the side surface

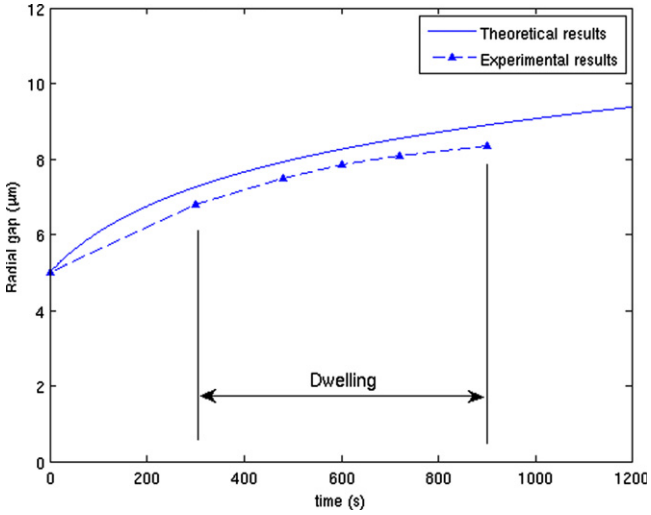

Fig. 10. Change of radial gap over time (*frequency*=500 kHz, *duty ratio*=0.3).

of micro-hole, as exhibited in Fig. 8. For micro-hole shown in Fig. 8a, the re-solidified material could be seen on the rim and the overlapped discharge craters still exist on the lateral side surface. In contrast, the side surface of micro-hole in Fig. 8b is found to be smooth with no visible crater. This is due to the fact that a layer of affected material on machined surface is further dissolved by electrochemical reaction.

Fig. 9 compares the experimental results and theoretical results of radial gap for different duty ratio and frequencies. The feed rate is set at 0.2 μm/s for all experimental sets and the machining time is approximately 14 min for all micro-holes. For the machining time of micro-EDM alone, it is determined to be around 4 min by using short voltage pulses and high feed rate to suppress the effect of electrochemical reaction. Therefore, the dissolution time is expected to be 10 min. However, the radial gap investigated in this study is based on the average value of the top and bottom diameter of micro-holes. Hence, the dissolution time is presumed to 5 min for simulation. It can be observed in Fig. 9 that there is a reasonable agreement between the simulated data and the experimental results for all the frequencies 100, 300 and 500 kHz. It is found to be in accordance with the aforementioned analysis in which the radial gap is increased when higher pulse duty ratio is used. In addition, the obtained experimental results also show that the radial gap is slightly smaller when higher frequency is applied. This is also consistent with the rational explanation described in Section 3.3.

To further demonstrate the effectiveness of short voltage pulses in localizing the material dissolution zone, the radial gap is investigated when micro-hole is exposed to long dissolution time. After finishing the drilling of micro-hole, the electrode is forced to dwell at that position for additional certain duration instead of being retracted. Fig. 10 outlines the change of radial gap over time and compares them with the theoretical results. It could be observed that the experimental results have the same increasing trend with the simulated data. Especially, although undergoing dissolution for additional duration as long as 600 s, the radial gap is found to increase 1.5 μm only. Moreover, from the experimental results, it could be obtained that the dissolution rate significantly drops from around 0.004 μm/s at the start of the dwelling period to 0.0015 μm/s at the end point of dwelling time. This is in accordance with the analysis in Section 3.2. With the limited voltage pulse width, the double layer is merely charged within a certain distance which results in the localization of dissolution zone. This confirms the effectiveness of short voltage pulses in maintaining high dimensional accuracy for SEDCM.

5. Conclusions

This study attempts to perform the analytical modeling of radial gap distance in simultaneous micro-EDM and micro-ECM drilling and verify it with experimental results. The following conclusions could be drawn from this study:

a. In SEDCM drilling, a thin layer of affected material on the lateral surface of micro-hole is further dissolved by electrochemical reaction whereby its surface integrity is improved.
b. The material dissolution in low-resistivity deionized water could be modeled using the double layer theory, Butler–Volmer equation and Faraday's law of electrolysis.
c. Pulse parameters such as frequency and duty ratio directly affect the thickness of affected material layer further dissolved from inner surface of micro-holes.
d. Owing to double-layer charging characteristic, short voltage pulses are effective in localizing the material dissolution zone and thus maintain high dimensional accuracy for SEDCM.
e. When the pulse duration is too short, the material dissolution is negligible and SEDCM has no effect on improving the surface finish of micro-hole.

There is reasonable agreement between the simulated data and experimental results. The presented approach is thus useful for determining suitable machining condition and predicting the dimension of micro-holes.

References

[1] L. Uriarte, A. Herrero, A. Ivanov, H. Oosterling, L. Staemmler, P.T. Tang, D. Allen, Comparison between microfabrication technologies for metal tooling, Proceedings of the Institution of Mechanical Engineers, Part C, Journal of Mechanical Engineering Science 220 (2006) 1665–1676.
[2] E. Uhlmann, S. Piltz, U. Doll, Machining of micro/miniature dies and moulds by electrical discharge machining—recent development, Journal of Materials Processing Technology 167 (2005) 488–493.
[3] P. Bleys, J.P. Kruth, B. Lauwers, B. Schacht, V. Balasubramanian, L. Froyen, J. Van Humbeeck, Surface and sub-surface quality of steel after EDM, Advanced Engineering Materials 8 (2006) 15–25.
[4] B. Ekmekci, A. Sayar, T.T. Öpöz, A. Erden, Geometry and surface damage in micro electrical discharge machining of micro-holes, Journal of Micromechanics and Microengineering 19 (2009) 105030.
[5] P.C. Tan, S.H. Yeo, Modelling of overlapping craters in micro-electrical discharge machining, Journal of Physics D: Applied Physics 41 (2008) 205302.
[6] B. Bhattacharyya, J. Munda, M. Malapati, Advancement in electrochemical micro-machining, International Journal of Machine Tools and Manufacture 44 (2004) 1577–1589.
[7] T. Masuzawa, S. Sakai, Quick finishing of WEDM products by ECM using a mate-electrode, CIRP Annals—Manufacturing Technology 36 (1987) 123–126.
[8] T. Masuzawa, M. Kimura, Electrochemical surface finishing of tungsten carbide alloy, CIRP Annals—Manufacturing Technology 40 (1991) 199–202.
[9] K. Takahata, S. Aoki, T. Sato, Fine surface finishing method for 3-dimensional micro structures, Proceedings of IEEE Micro Electro Mechanical Systems (MEMS) (1996) 73–78.
[10] T. Kurita, M. Hattori, A study of EDM and ECM/ECM-lapping complex machining technology, International Journal of Machine Tools and Manufacture 46 (2006) 1804–1810.
[11] T. Masuzawa, C.L. Kuo, M. Fujino, A combined electrical machining process for micronozzle fabrication, CIRP Annals—Manufacturing Technology 43 (1994) 189–192.
[12] D.K. Chung, H.S. Shin, B.H. Kim, M.S. Park, C.N. Chu, Surface finishing of micro-EDM holes using deionized water, Journal of Micromechanics and Microengineering 19 (2009) 045025.
[13] D.K. Chung, B.H. Kim, C.N. Chu, Micro electrical discharge milling using deionized water as a dielectric fluid, Journal of Micromechanics and Microengineering 17 (2007) 867–874.
[14] Z. Zeng, Y. Wang, Z. Wang, D. Shan, X. He, A study of micro-EDM and micro-ECM combined milling for 3D metallic micro-structures, Precision Engineering 36 (2012) 500–509.
[15] M.D. Nguyen, M. Rahman, Y.S. Wong, Simultaneous micro-EDM and micro-ECM in low-resistivity deionized water, International Journal of Machine Tools and Manufacture 54–55 (2012) 55–65.
[16] M.D. Nguyen, M. Rahman, Y.S. Wong, Enhanced surface integrity and dimensional accuracy by simultaneous micro-ED/EC milling, CIRP Annals-Manufacturing Technology 61 (1) (2012) 191–194.
[17] C.C. Kao, J. Tao, A.J. Shih, Near dry electrical discharge machining, International Journal of Machine Tools and Manufacture 47 (2007) 2273–2281.
[18] K.H. Schoenbach, J.F. Kolb, S. Xiao, S. Katsuki, Y. Minamitani, R.P. Joshi, Electrical breakdown of water in microgaps, Plasma Sources Science and Technology 17 (2008) 024010.
[19] J.F. Kolb, R.P. Joshi, S. Xiao, K.H. Schoenbach, Streamers in water and other dielectric liquids, Journal of Physics D: Applied Physics 41 (2008) 234007.
[20] R. Schuster, V. Kirchner, P. Allongue, G. Ertl, Electrochemical Micromachining, Science 289 (2000) 98–101.
[21] A.J. Bard, L.R. Faulkner, Electrochemical Methods: Fundamentals and Applications, second ed., John Wiley, New York, 2001.
[22] O. De Abril, A. Gündel, F. Maroun, P. Allongue, R. Schuster, Single-step electrochemical nanolithography of metal thin films by localized etching with an AFM tip, Nanotechnology 19 (2008) 325301.
[23] J. Kozak, D. Gulbinowicz, Z. Gulbinowicz, The mathematical modeling and computer simulation of pulse electrochemical micromachining, Engineering Letter 16 (2008) 556–561.